13th Australasian Fluid Mechanics Conference
Monash University, Melbourne, Australia
13-18 December 1998

The Effects of Impeller Exit Rake Angle on the Internal Flow of Centrifugal Impellers

Ichiro Ariga
Chiba Institute of Technology
2-17-1 Narashino, Chiba-Pref. JAPAN 275-0016
Makoto Umezawa
Nissan Motor Co., Ltd.
560-2 Okatsukoku, Atsugi, Kanagawa, JAPAN 243-0192

ABSTRACT

In this study, within the various aspects of the aerodynamic performance of the three-dimensional impeller, the effects of the rake angle of impeller blade exits on leakage through the shroud side clearance of impeller were investigated. We produced three distinct varieties of impeller, with rake angles at 0°, 20°, and 40°.

At the same time, we altered the shroud side clearances and attempted to investigate the influence on performance as well as on leak flow.

As a result, it was recognized that the appropriate rake angle yielded higher performance around low flow rate range, and reduced leakage through the shroud side clearance of an impeller.

INTRODUCTION

There has been considerable progress in the development of centrifugal fans and compressors in their various uses in industrial plants, turbo-chargers and gas turbines. In recent years in particular, streamline analysis theory and applied an analysis technology have made great strides, and advances in manufacturing technology have made it possible to produce complex three-dimensional impellers that are characterized by high efficiency over a wide range of flow rate.

Much research has been reported, concerning such three-dimensional impellers with a rake angle, the impeller in the outlet section being so configured that blades are leaned towards the rotating direction(Vanek, 1983, Polak and Roberts, 1986).

Several studies about the influence of leakage on the impeller performance have been also reported (Farge, et. al, 1989). However the effects of blade rake angle on leakage from the shroud side clearance in the impeller have not been adequately clarified.

In the present study, configuration parameters other than those for the rake angle at the exit were devised the same. The goal was to extract the effect of the rake angle alone. Thus three distinct varieties of impeller, with rake angles at 0°, 20°, and 40° were manufactured. At the same time, we altered the shroud side clearances and attempted to investigate its influence on leakage. In the experiment, we measured the distribution of static pressure on the shroud wall, the leak flow in the shroud clearance and the velocity distribution of discharge flow out of the impeller. We also investigated, by means of certain visual methods, the effect of the rake angle on the impeller's internal flow. The influence on performance was also studied.

EXPERIMENTAL APPARATUS AND PROCEDURES

Fig. 1 shows the complete experimental apparatus. The side clearance between the blade tips and the shroud casing of an impeller are adjustable at 0.5mm intervals over 0.5mm～7.5mm by inserting washers in the clearance of the impeller casing and the screws to adjust the diffuser exit width. Fig. 2 shows the impellers with rake angles at R=0°, 20° and 40° used in the present experiment. The specifications of the impeller and diffuser are shown in Table 1. The radial blade impeller was used to find only the effects of the blade rake angles. In the experiment the rotational speed was maintained at n=1, 330 rpm and the flow rate was measured by means of a nozzle-flow meter set on the inlet duct.

The flow coefficient ϕ is obtained as follows,

$$\phi = Q/(S \cdot U_2)$$

, where Q is corrected volume flow rate [m^3/s], S is sectional area at the impeller exit [m^2] and U_2 is peripheral velocity at the impeller exit [m/s].

The measurements of static pressure were made by the taps on the shroud casing and then the discharge flow distribution out of the impeller by the slant hot wire anemometer and leak flow in the clearance between the blade tips and the shroud casing were measured by means of an I-type hot wire sensor. Furthermore, leak flow behavior was also observed by means of a visual method where smoked paraffin was injected into the flow within the impeller. The injection taps on the blade surface are shown in Fig. 11.

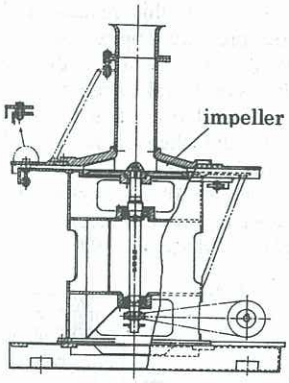

Fig.1 Experimental apparatus

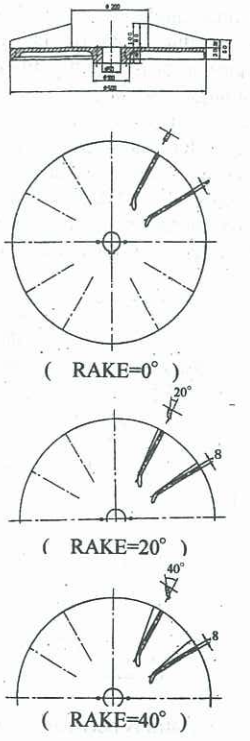

Fig.2 Centrifugal impeller

Type	Radial Fan
Rotational Speed	0 rpm ～ 2000 rpm
Impeller Outlet Rake Angle	0°, 20°, 40°
Outer Diameter of Impeller	0.5 m
Inner Diameter of Impeller	0.2 m
Blade Height at Impeller Outlet	0.02 m
Blade Height at Impeller Inlet	0.06 m
Blade Angle at Impeller Outlet	90 °
Blade Angle at Impeller Inlet	34 °
Numbers of Blade	12
Blade Thickness	0.008 m
Flow Coefficient at Design Point	0.3
Diffuser Type	Vaneless Diffuser
Outer Diameter of Diffuser	1 m
Inner Diameter of Diffuser	0.5 m

Table 1 Specification of Test Fan

EFFECT OF RAKE ANGLES ON PERFORMANCE

Fig. 3 shows the variations of the static pressure coefficient ϕ against the flow coefficient ϕ and the static pressure coefficient is expressed as

$$\phi = (P_s - P_a)/(\rho U_2^2/2)$$

where P_s is atatic pressure [Pa], P_a is atomospheric pressure [Pa] and ρ is air density [kg/m^3].
The side clearance of the impeller is represented as

$$\lambda = Z/b_2$$

, where Z is side clearance [m], and b_2 is blade width at the impeller exit [m].
The experiments were conducted with λ =0.025, 0.10, 0.15 for each rake angle at n=1, 330rpm. From this relation it is observed that a drops in static pressure appears as side clearance increases, but influence due to clearance is difficult with a larger rake angle. The effects of the rake angle for each clearance was also studied and it was clarified that the static pressure decreases as λ increases and then there is little difference in static pressure for varied rake angles.
In the case of λ =0.025 and rake angle R=20°, the performance improves in the lower flow rate range and we can recognize the same tendency in other results (Fig. 4) (Maekawa, 1988).

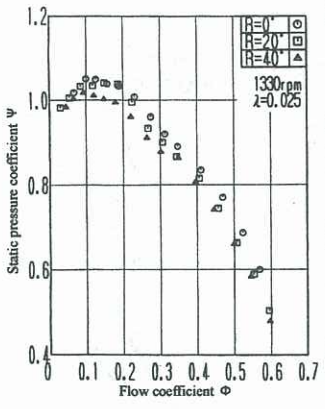

Fig. 3 Relations between flow coefficient and static pressure coefficient

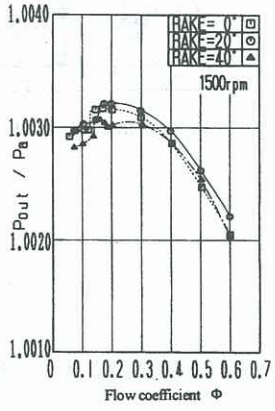

Fig. 4 Performance curve

VELOCITY DISTRIBUTION AT IMPELLER EXIT

The flow pattern out of the impeller was investigated to compare the differences yielded by the different rake angles. The experiment in which velocity was measured by a slant hot wire anemometer at the site in Fig. 5 was carried out, varying the clearance λ =0.025, 0.05, 0.10 and 0.15 for ϕ =0.3, 0.4, 0.5 at n=1, 330rpm.
Fig. 5 shows the non-dimensional radial velocity component of discharge flow, Cr_2/U_2 at ϕ =0.3, where Cr_2 is the radical velocity component. In this case, the reverse flow region appears around the shroud side of the impeller and this region increases as the rake angle increases. The velocity near the hub side becomes higher with increase of the rake angle and thus the difference of velocities at the shroud and hub sides becomes excessively large and the velocity profiles are skewed. With regard to thus, the flow angle at the impeller exit was measured.
Fig. 6 shows the yew angle ξ of discharge flow versus measuring sites from the hub surface of the impeller. We can also see that variation of ξ in the shroud side clearance is larger for R=40° than for R=0° and 20°. Accordingly, the strong skew of discharge flow for too large rake angle can be verified. It is observed that in the case of λ =0.025, the discharged wake regions which are generated by the secondary flow developed within the impeller passage are shifted a little from the pressure side to the suction side with an increase in rake angle, because the leak flow in the clearance toward the pressure side from the suction side of the blade decreases due to the increment of the rake angle. The secondary flow originating from leakage becomes weaker and this weak region is made to move to the suction side surface.

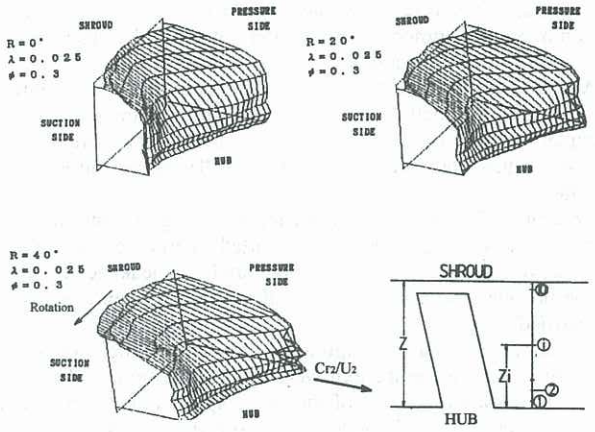

Fig. 5 Meridional velocity distribution at impeller exit(Slant hot wire)

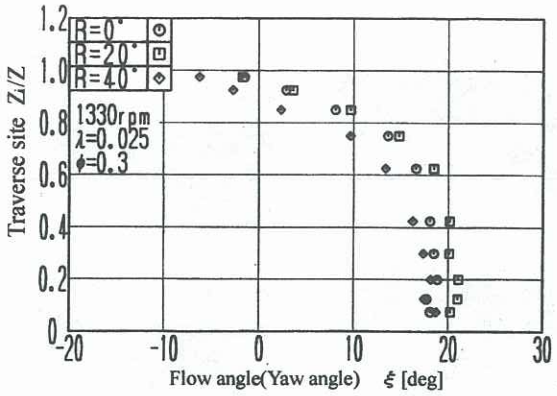

Fig. 6 Flow Angle Distribution at Impeller Exit

STATIC PRESSURE DROPS BASED ON CLEARANCE

Fig. 7 shows the drop in static pressure due to the shroud side clearance obtained from pressure measured upon the shroud casing surface. It is plotted as the relation of the static pressure drop $-\triangle \phi$ versus the non-dimensional distance Li/L in which L is the whole blade length and L_i is the length from the blade inlet to any point along the center line on the meridional blade surface.

$-\triangle \phi$ is represented as follows:

$$-\triangle \phi = (\phi_{min} - \phi) - (\phi_{min1} - \phi_1)$$

, where ϕ_{min} is static pressure coefficient with λ =0.025 at any measuring point, ϕ is static pressure coefficient with a certain λ at the same point and ϕ_{min1} is static pressure coefficient with λ =0.025 at L_i/L=0, ϕ_1 is static pressure coefficient with a certain λ at L_i/L=0.

The static pressure drop was evaluated, varying ϕ and λ for each rake angle. Fig. 7 is one case of them. As a result, the static pressure drop at the impeller exit increases with a larger clearance, and the difference between λ =0.10 and 0.15 is reduced due to a larger rake angle. The shroud side clearance thus hardly affects on the pressure drop as the rake angle increases.

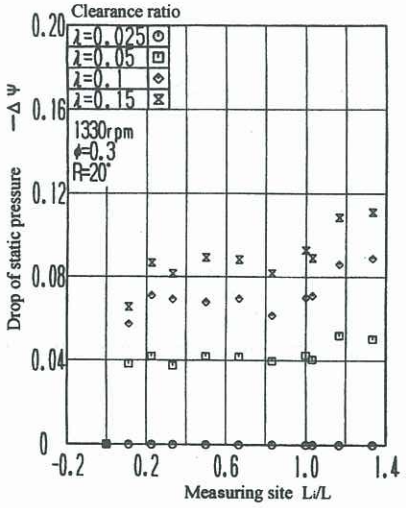

Fig.7 Drops of static pressure based on shroud side clearance

VELOCITY DISTRIBUTION IN SHROUD SIDE CLEARANCE

The peripheral velocity component of leak flow through the gaps between the blade tips and the shroud casing was measured by an I-type hot wire sensor in the sites shown in Fig. 8. The experiment was performed in the condition of ϕ =0.3, 0.4, 0.5 and λ =0.05, 0.10, 0.15, keeping n=1, 330rpm.

Fig. 9 shows the velocity in some cases of them. In this figure, there appears only a slight difference for any rake angle in the neighborhood of the impeller inlet (L_i/L=0.23).

In the middle part of the impeller passage, the variations according to rake angle are observed and the leak velocity is gradually reduced from the blade tips to the shroud wall with a larger angle. Just around the impeller exit (L_i/L=0.83), the reduction of leak velocity becomes more remarkable, due to the increment in rake angle. The same tendency is found, even if the flow rate changes. On the other hand, the difference between R=20° and 40° is barely detectable.

As mentioned above, the effects of rake angle on the leak flow is remarkable in the case of smaller clearance. while as clearance increases, the regions influenced by the pressure difference between the pressure side and the suction side are limited to the area near the blade tips. In the other region, the effect of clearance on leak flow disappears, as the pressure difference is unified in the clearance space.

Fig. 10 shows the leak flow rate $\triangle$Q, which was evaluated as an integrated amount from the leak velocity distribution and is plotted on the ordinate, where the velocity on the shroud wall is defined as 1 and on the blade tip as 0.

From these results, though the difference in flow rate due to different rake angles is barely perceptible near the impeller inlet, the leak flow decreases downstream in the impeller. Such a tendency becomes stronger toward the impeller exit.

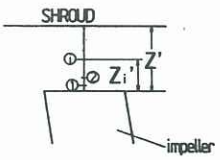

Fig.8 Measuring Position in Shroud (I-type hot wire)

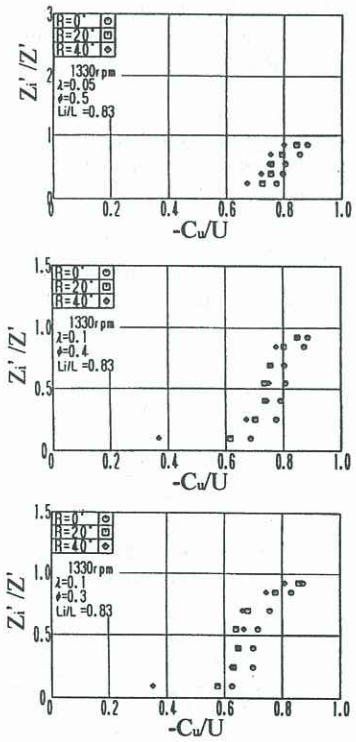

Fig.9 Velocity distribution In shroud clearance

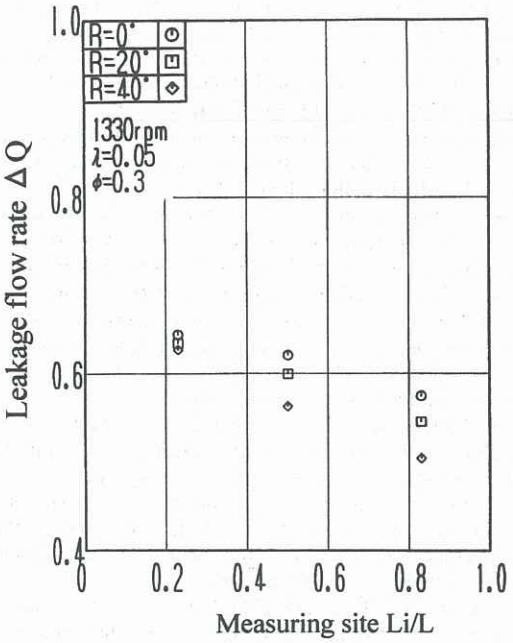

Fig. 10 Leak flow rate through shroud side clearance

FLOW BEHAVIOR THROUGH SIDE CLEARANCE BY VISUALIZATION

Fig. 12 shows a photograph by the visualized method, and the visualization system in Fig. 11 was employed. The experiment was performed with ϕ =0.3 and n=1,000rpm, with λ varying at 0.025, 0.10 and 0.15. The photograph shows only one case of λ =0.1 for the pressure surface here. In this photograph, the behavior of leak flow can be observed in the state of inflow into the suction side from the pressure side through the gaps between the shroud casing and the blade tips. On that occasion the leakage increases when the clearance ratio changes from λ =0.025 to 0.10, while there is little difference in the case of λ =0.10 and 0.15. It is also conceivable that at every clearance ratio the leakage of smoke into the suction side from the pressure side is weakened and remains to flow out downstream. On the other hand, the leakage behavior near the suction side changes little despite the different rake angle.

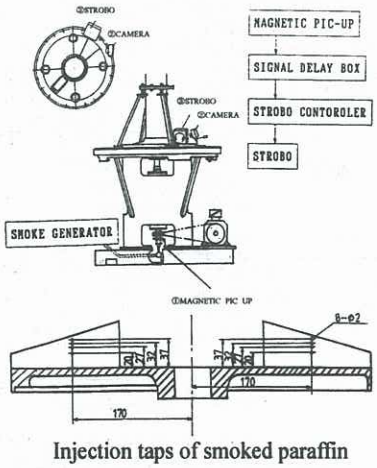

Injection taps of smoked paraffin

Fig. 11 Visualization system

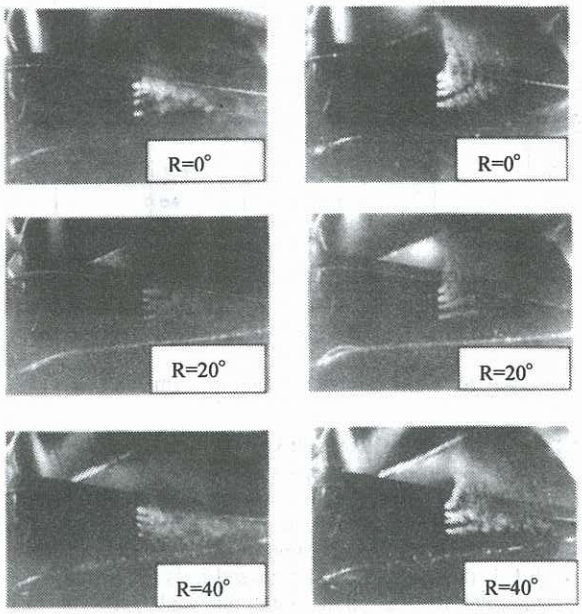

(λ =0.025, ϕ =0.3) (λ =0.1, ϕ =0.3)

Fig. 12 Leakage flow observed by smoked paraffin (Pressure surface)

CONCLUSION

Because of high performance, three-dimensional impellers have been recently used in many actual applications. These impellers are usually manufactured as blades with a rake angle at the impeller exit and very little has been reported about their effect on performance.

In the present study, the effects of the blade rake angle on leakage through the shroud side clearance were examined, using test impellers with three kinds of rake angle. The following effects occurred as the rake angle increased.

1) Leak flow rate through the shroud side clearance was reduced. This tendency became remarkable as clearance was smaller.
2) Secondary flow at the impeller exit due to leak flow reduced as a consequence of the decrease of leakage within the impeller.

As a result, it was concluded that an impeller with an appropriate rake angle prevents leakage and thus has a good effect upon impeller performance directly and/or indirectly.

REFERENCES

Vanek, V., "Contribution to Centrifugal Compressor Impeller Design, "AIAA Paper, 83-7064, P-563, 1983.

Polak, P. and Roberts, B. D., "Improving Flow Distribution in Centrifugal Compressors", Proc. Int. Mech. Engrs., 200, A1, P-59, 1986

Farge, T. Z., Johnson, M. W. and Maksound, T. M. A., "Tip Leakage in a Centrifugal Impeller", Trans. ASME, 111. P-244, 1989

Maekawa, Y., "The Effects of Impeller Configuration on Performance, "KEIO Univ. Master Thesis, 1988